Cell Research (2012) 22:346-359.

www.nature.com/cr

ORIGINAL ARTICLE

The p97 ATPase associates with EEA1 to regulate the size of early endosomes

Harish N Ramanathan[1], Yihong Ye[1]

[1]*Laboratory of Molecular Biology, National Institute of Diabetes and Digestive and Kidney Diseases, National Institutes of Health, Bethesda, MD 20892, USA*

The AAA (ATPase-associated with various cellular activities) ATPase p97 acts on diverse substrate proteins to partake in various cellular processes such as membrane fusion and endoplasmic reticulum-associated degradation (ERAD). In membrane fusion, p97 is thought to function in analogy to the related ATPase NSF (N-ethylmaleimide-sensitive fusion protein), which promotes membrane fusion by disassembling a SNARE complex. In ERAD, p97 dislocates misfolded proteins from the ER membrane to facilitate their turnover by the proteasome. Here, we identify a novel function of p97 in endocytic trafficking by establishing the early endosomal autoantigen 1 (EEA1) as a new p97 substrate. We demonstrate that a fraction of p97 is localized to the early endosome membrane, where it binds EEA1 via the N-terminal C2H2 zinc finger domain. Inhibition of p97 either by siRNA or a pharmacological inhibitor results in clustering and enlargement of early endosomes, which is associated with an altered trafficking pattern for an endocytic cargo. Mechanistically, we show that p97 inhibition causes increased EEA1 self-association at the endosome membrane. We propose that p97 may regulate the size of early endosomes by governing the oligomeric state of EEA1.

Keywords**:** p97/VCP/Cdc48; EEA1; AAA ATPase; early endosome; endocytosis

Cell Research (2012) **22**:346-359. doi:10.1038/cr.2011.80; published online 10 May 2011

Introduction

The p97 (also named Cdc48 in yeast) is an evolutionarily conserved AAA ATPase. It contains two Walker-type ATPase domains that are assembled into a hexameric ring with a central pore [1, 2]. It is thought to function as an ubiquitin-selective chaperone to segregate substrate proteins from large immobile cellular complexes, such as the ER membrane, chromatin and microtubule. Accordingly, p97/Cdc48 has been demonstrated to act in variable cellular settings including endoplasmic reticulum-associated protein degradation (ERAD), DNA replication, transcription regulation, the formation of nuclear envelop, spindle disassembly, and the homotypic fusion of ER/Golgi membranes [3-7]. The functional flexibility of p97/Cdc48 is hinged on the various cofactors that bind p97 via its N-terminal domain. In ERAD, the p97 cofactor complex Ufd1-Npl4 assists p97 in substrate recognition and dislocation from the ER membrane [3, 4, 8]. In homotypic fusion of the ER [9-11] and the Golgi [12-14], p97 acts on a yet to be identified substrate in conjunction with the cofactor p47 and the p37-VCIP135 complex. Thus, adaptor selection appears to dictate the enrollment of p97 into different cellular pathways [4, 15]. In this regard, it is interesting to note that the endocytic adaptor protein clathrin was the first identified p97-interacting protein [16]. Nonetheless, whether p97 plays a role in endocytic regulation has remained unclear.

During endocytosis, internalized vesicles constantly fuse to form early endosomes, which migrate toward the center of the cell while maturing into the MVB compartment. Endocytic vesicle docking and fusion require cooperation between many soluble and membrane components. Among them, the early endosome-associated autoantigen 1 (EEA1) is an essential component that

Correspondence: Yihong Ye
Tel: +301-5940845; Fax: +301-4960201
E-mail: yihongy@mail.nih.gov
Abbreviations: ERAD (endoplasmic reticulum-associated degradation); EEA1 (early endosomal antigen1); NEM (N-ethylmaleimide); EerI (eeyarestatin I)
Received 15 November 2010; revised 9 March 2011; accepted 28 March 2011; published online 10 May 2011

dynamically distributes between an endosome membrane-associated and a soluble cytosolic form [17-20]. Membrane association of EEA1 is regulated by the Rab5 GTPase, a master regulator of endocytic trafficking [21-23]. Once localized to the endosome membrane, EEA1 serves as a tethering factor to link endocytic vesicles to early endosomes for fusion catalyzed by a SNARE complex and N-ethylmaleimide-sensitive fusion protein (NSF) [20, 24, 25]. Distinct structural elements within EEA1 confer on it the ability to dock and tether vesicles. The carboxyl-terminus of EEA1 carries a FYVE domain responsible for binding to phosphatidyl inositol-3-phosphate on the membrane [19, 20, 26-28]. The N-terminal C2H2 zinc finger domain and a region upstream of the FYVE domain serve as Rab5-binding sites [21]. EEA1 also harbors a calmodulin-binding (IQ) domain and a long helical segment [17]. The latter is responsible for the homodimerization of EEA1, which is thought to be a prerequisite for the tethering function [28, 29]. In cells, Rab5 activation leads to the complex of the EEA1 dimer into a large protein complex that contains other Rab5 effectors such as the Rab5 GTP exchange factor Rabex-5 and Rabaptin-5 as well as the endosome-specific t-SNARE Syntaxin-13, which results in the fusion of endosomes [24].

In this study, we took an unbiased biochemical approach to identify EEA1 as a new substrate of p97. Our results indicate that p97 may regulate the oligomeric state of EEA1 to influence its membrane-tethering function, which in turn affects the size of early endosomes. These findings for the first time establish the AAA ATPase p97 as a key regulator of endocytic protein trafficking.

Results

The p97 is localized to the endosomes and interacts with EEA1

The p97 is localized in the cytosol, nucleus and also on the ER membrane [4]. Accordingly, when total membranes from 293T cells were analyzed by a floatation assay using a sucrose gradient, most membrane-bound p97 remained at the bottom of the gradient (Figure 1A), which contained the ER and other heavy membranes, as demonstrated previously [30]. However, a substantial amount of p97 was also bound to light membranes enriched with the early endosomal protein EEA1 and the endosome/lysosome marker LAMP1 (Figure 1A), indicating that p97 may also associate with endosomes.

To identify endosomal proteins that bind p97, we purified p97 from detergent extract of endosome-enriched cow liver total membrane fraction using a p97-specific antibody. IgG was used as a negative control. SDS-PAGE analysis revealed a major band of ~180 kD co-purified with p97 as well as several minor bands. Mass spectrometry analysis identified two proteins present in the 180 kD band, the mitochondrial carbamoyl-phosphate synthase (CPSM) and EEA1 (Figure 1B and Supplementary information, Figure S1). Given the observed association of p97 with endosomes, we further characterized the p97-EEA1 interaction.

We first confirmed the EEA1-p97 interaction in 293T cells using co-immunoprecipitation (co-IP) analysis. Immunoblotting showed that the anti-p97 antibody but not control IgG specifically precipitated p97 together with endogenous EEA1 (Figure 1C). The interaction could be reproduced using HeLa cell extract (Figure 1D). Because p97 belongs to a subfamily of AAA ATPases that are sensitive to the cysteine-specific alkylating agent N-ethylmaleimide (NEM), we also examined whether NEM could affect the EEA1-p97 interaction. Our results showed that the addition of NEM to cell extracts significantly reduced the association of EEA1 with p97, likely due to dissociation of EEA1 from NEM-inactivated p97 (Figure 1D).

To further confirm this interaction in living cells, we used confocal microscopy to examine the colocalization of p97 with EEA1 on endosomes in COS7 cells. Given the small size of early endosomes in normal cells and the ubiquitous nature of p97 expression, an assessment of colocalization between these two proteins on wild-type endosomes proved to be cumbersome. To circumvent this, we expressed a constitutively active Rab5 mutant (Q79L). Q79L bound EEA1 constitutively, resulting in enrichment of EEA1 on endosomal membranes and enlargement of early endosomes [20, 31]. We hypothesized that if p97 interacted with EEA1, Q79L expression should lead to accumulation of p97 on these enlarged endosomal structures to a higher level than the cytosolic p97 background. Our results showed that endogenous p97 was indeed enriched to the enlarged endosomes in cells expressing the Rab5 Q79L mutant (Figure 1E). Given that EEA1 could be co-precipitated with p97 (Figure 1C and 1D), the most plausible explanation for the immunostaining data is that a fraction of p97 is localized to the early endosomes where it binds EEA1.

The C2H2 domain in EEA1 is required for p97 association

EEA1 contains several established functional domains as depicted in Figure 2A. To understand how p97 interacts with EEA1, we mapped the domain in EEA1 required for binding to p97. We used a human EEA1 full-length expression clone with a carboxyl-terminal FLAG tag. When FLAG-tagged EEA1 was expressed in cells, it displayed a similar localization pattern as endogenous

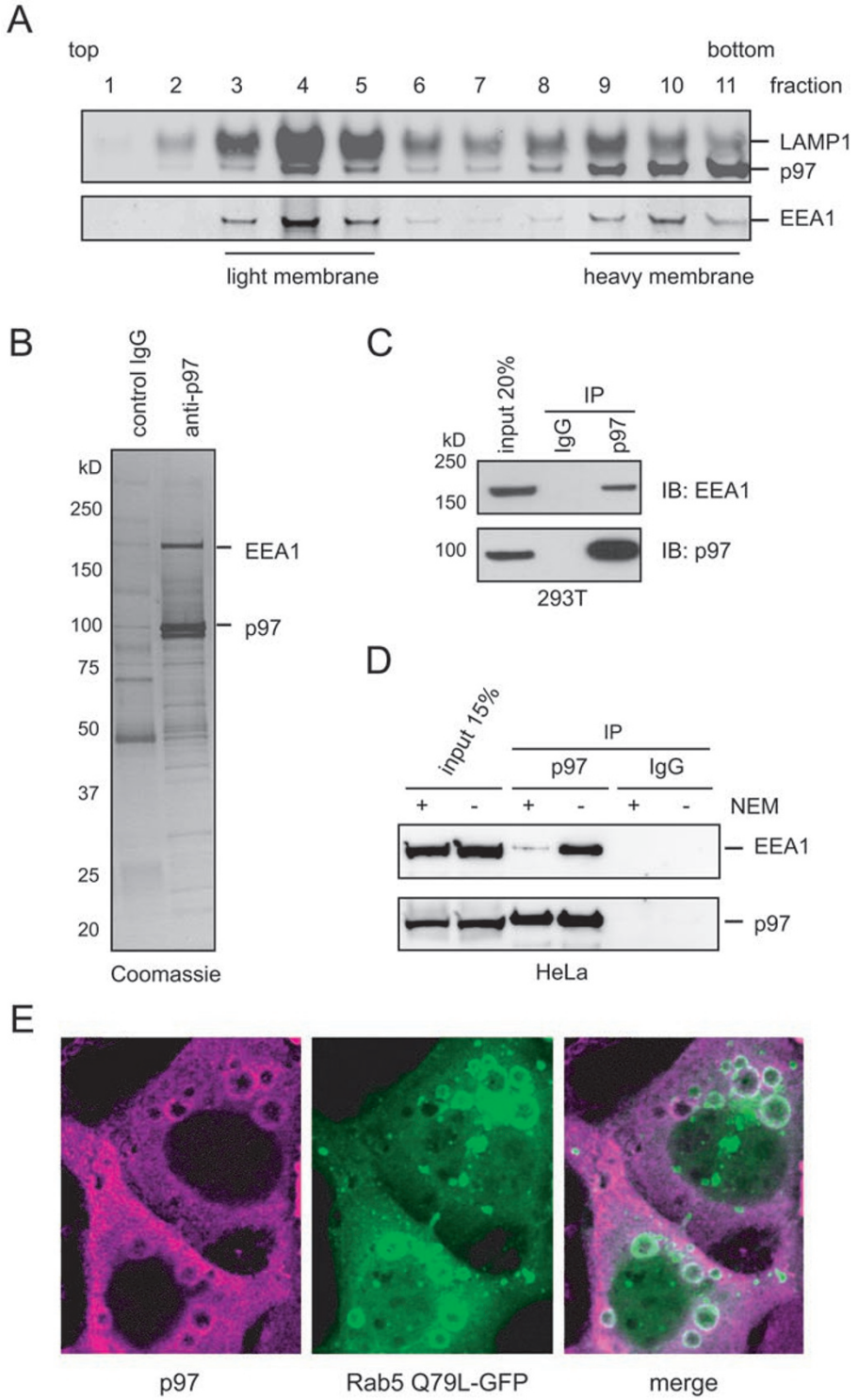

Figure 1 The p97 is localized to the endosomes and interacts with EEA1. **(A)** A post nuclear supernatant fraction from 293T cells was subject to sucrose gradient floatation to separate membranes based on their density. Collected fractions were analyzed by immunoblotting with the indicated antibodies. **(B)** A Coomassie blue stained gel showing proteins co-purified with p97 from solubilized cow liver membrane. **(C)** Co-IP analysis of EEA1-p97 interaction using 293T cell extracts. **(D)** As in **C**, except that HeLa cells were used. Where indicated, cell extracts were treated with 5 mM NEM. **(E)** Confocal analyses of COS7 cells showing endogenous p97 (left panel), overexpressed Rab5 (Q79L) GFP (middle) and the merged image (right).

EEA1 (data not shown) and it could be co-precipitated with p97 (Figure 2B). We then generated and expressed several truncated EEA1 mutants in cells. Co-IP experiments demonstrated that deletion of the N-terminal 69 amino acids from EEA1 was sufficient to abolish p97 interaction. In contrast, deletion of the C-terminal FYVE domain did not affect the binding (Figure 2B). These data indicate that the N-terminal C2H2 domain is required for EEA1 binding to p97. Moreover, because the FYVE domain is required for association of EEA1 with the endosome membrane, the fact that its absence does not compromise the p97-EEA1 interaction indicates that p97 may bind EEA1 both on the endosome membrane and in the cytosol.

Because co-immunoprecipitation experiments using purified EEA1 and p97 failed to reveal a direct interaction (data not shown), we assumed that the interaction of p97 with EEA1 might be mediated by a p97 cofactor in cells. To date, a large number of p97 cofactors have been identified [32]. Among them, the best-characterized ones are a dimeric complex comprising Ufd1 and Npl4 [33], which assists p97 in degradation of misfolded ER proteins [34], and p47, which facilitates p97 function in homotypic fusion of Golgi membranes [35]. We tested whether these p97 cofactors were involved in EEA1-p97 interaction. We postulated that overexpression of a cofactor that mediates the interaction of p97 with EEA1 should increase p97-EEA1 association. However, neither the Ufd1-Npl4 complex nor p47 could enhance the association of p97 with EEA1 (Supplementary information, Figure S2), suggesting that other cofactors may be involved in this interaction.

The p97 inhibition results in enlargement of early endosomes

To examine the potential function of p97 in regulating early endosome morphology and/or trafficking, we first used a p97-specific siRNA to deplete p97 from cells. The siRNA treatment of COS7 cells reduced the p97 protein levels by more than 80% when compared to a control

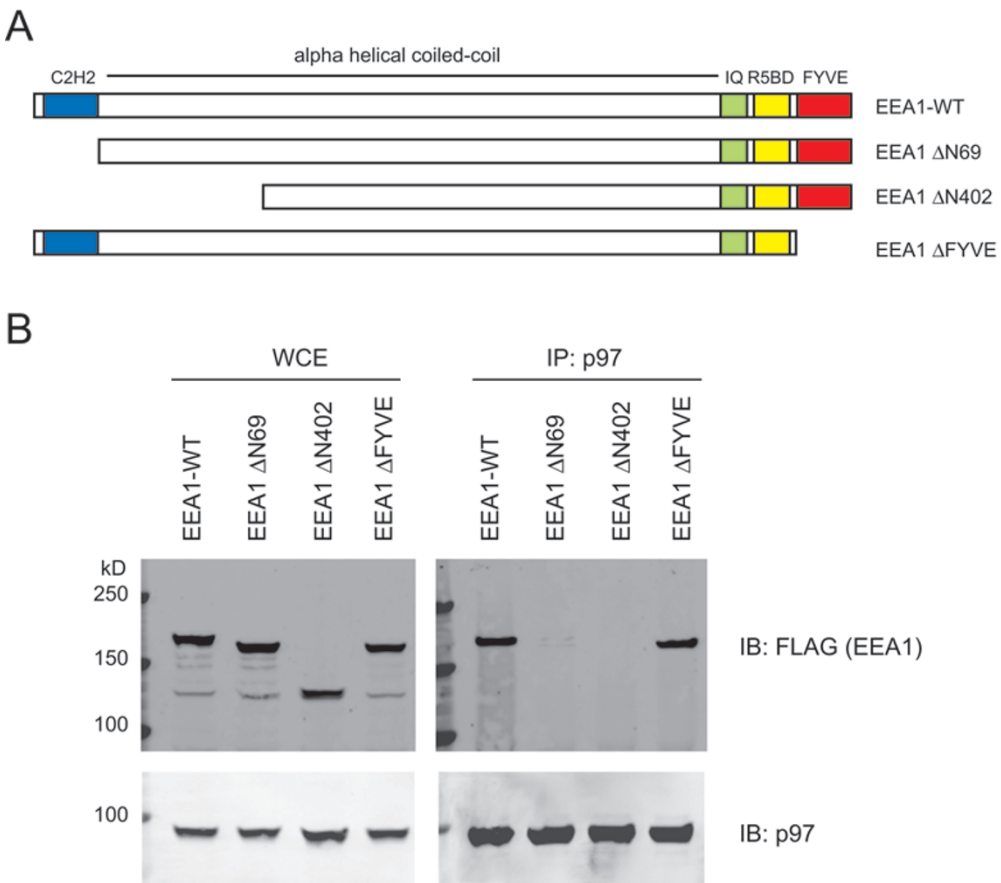

Figure 2 The C2H2 domain in EEA1 is required for p97 association. **(A)** Schematic representation of full-length EEA1 and the deletion constructs used in the binding study. IQ, calmodulin-binding site; R5BD, Rab5-binding domain. **(B)** Co-IP analysis of p97 interaction with the EEA1 variants. WCE, whole cell extract.

siRNA (Figure 3A). We then examined the early endosome morphology by immunostaining with an EEA1 antibody. Confocal microscopy revealed that p97 siRNA treatment resulted in enlarged early endosomes. In addition, p97 knockdown cells often contained clustered endosomes when compared to the control siRNA-treated cells (Figure 3B, panels 4-6 versus 1-3). Moreover, we also consistently observed increased EEA1 staining on endosomes in p97-depleted cells, although the level of membrane-associated EEA1 was unaltered (see below). To exclude the possibility that the observed phenotype was due to off-target effects of the p97 siRNA, we used a second p97 siRNA that could also deplete p97. Importantly, enlarged endosomes were also observed in cells treated with this siRNA (Supplementary information, Figure S3A).

Given that p97 is an essential regulator of ER protein homeostasis, we wished to rule out the possibility that the abnormality in endosome morphology associated with p97 knockdown was caused by impaired degradation of misfolded ER proteins. We used a siRNA to deplete Npl4 (Figure 3C), a p97 cofactor essential for ERAD. Consistent with previous reports [36, 37], knockdown of Npl4 inhibited ERAD, as indicated by the stabilization of the model ERAD substrate TCRα (Supplementary information, Figure S3B). Immunostaining showed that EEA1-positive early endosomes in Npl4 knockdown cells were indistinguishable from those in control cells (Figure 3D, panels 2, 5 versus panels 1, 4), whereas p97 depletion performed in parallel gave rise to obviously enlarged and clustered early endosomes (Figure 3D, panels 3, 6). These data suggest that the effect of p97 depletion on early endosomes does not result from disturbed ER protein homeostasis.

Since p97 co-fractionated with endosomes marked with both EEA1 and LAMP1, we asked whether p97 depletion also caused aberrant lysosome morphology. We stained control or p97 knockdown cells with a LAMP1 antibody. As shown in Figure 3E, no significant difference in size or distribution of the LAMP1-containing vesicles was evident between control and p97 siRNA-treated cells. Thus, p97 depletion appears to specifically influence the morphology of the EEA1-containing early endosomes.

To further examine the role of p97 in endocytosis, we assessed the effect of a p97 inhibitor on endosome morphology. Compared with the gene-silencing approach, chemical inhibitors can rapidly shut down protein function and thus allow observation of the immediate effect associated with loss of protein function. By contrast, siRNA experiments took several days and therefore the observed phenotype might be due to secondary effects downstream of prolonged p97 depletion. We recently characterized a small compound named eeyarestatin I (EerI), which preferentially interfered with the function of membrane-associated p97 [38]. Importantly, *in vitro* binding experiments showed that EerI did not bind to the highly related AAA ATPase NSF, making it a specific inhibitor of p97 [38].

Consistent with the siRNA results, treatment of COS7 cells with EerI for 6 h resulted in an apparent increase in endosome clustering and many enlarged endosomes compared to DMSO-treated cells (Figure 4A). Quantification of the size of vesicles showed that compared to control cells, the average diameter of endosomes in EerI-treated cells was increased by ~2-fold (Figure 4A). Moreover, like p97 knockdown cells, EEA1 staining intensity was significantly increased by EerI treatment (Supplementary information, Figure S3C).

To further characterize the endosome phenotype associated with p97 inhibition, we examined the endosome morphology in EerI-treated cells using Rab5-GFP, another well documented early endosome marker [39, 40]. Cells transiently expressing low levels of Rab5-GFP showed diffusive cytoplasmic localization of Rab5 as well as punctate Rab5-containing vesicles, as reported previously [41]. Transferrin (Tfn)-labeling experiment showed that the Rab5-containing vesicles could be labeled by Tfn (Supplementary information, Figure S4), suggesting that they represented *bona fide* endosome vesicles. In EerI-treated cells, Rab5-GFP-containing vesicles were enlarged and clustered (Figure 4B, panels 2, 4 versus panels 1, 3). Furthermore, transmission electron microscopy showed that EerI-treated cells contained many enlarged early endosome vesicles (Figure 4C versus Figure 4D). These results demonstrate that inhibition of p97 by EerI also leads to enlargement/clustering of endocytic vesicles, suggesting that p97 may regulate the docking or fusion of endosomes to govern their size.

Inhibition of p97 delays the trafficking of an endocytic cargo

To assess the functional consequence of p97 inhibition on endocytic trafficking, we monitored the transport kinetics of the endocytic cargo Tfn. To avoid indirect effect that could result from prolonged p97 inhibition, we treated cells with EerI for a short period of time (1 h). Cells were then incubated with fluorescence-labeled Tfn on ice. After removal of the unbound Tfn, the cells were chased in a medium free of Tfn at 37 ºC for different time periods. The cells were then fixed and processed for confocal imaging. In DMSO-treated cells Tfn initially labeled the plasma membrane, but it was soon internalized and the Tfn-containing vesicles migrated towards a perinuclear region and accumulated in the perinuclear

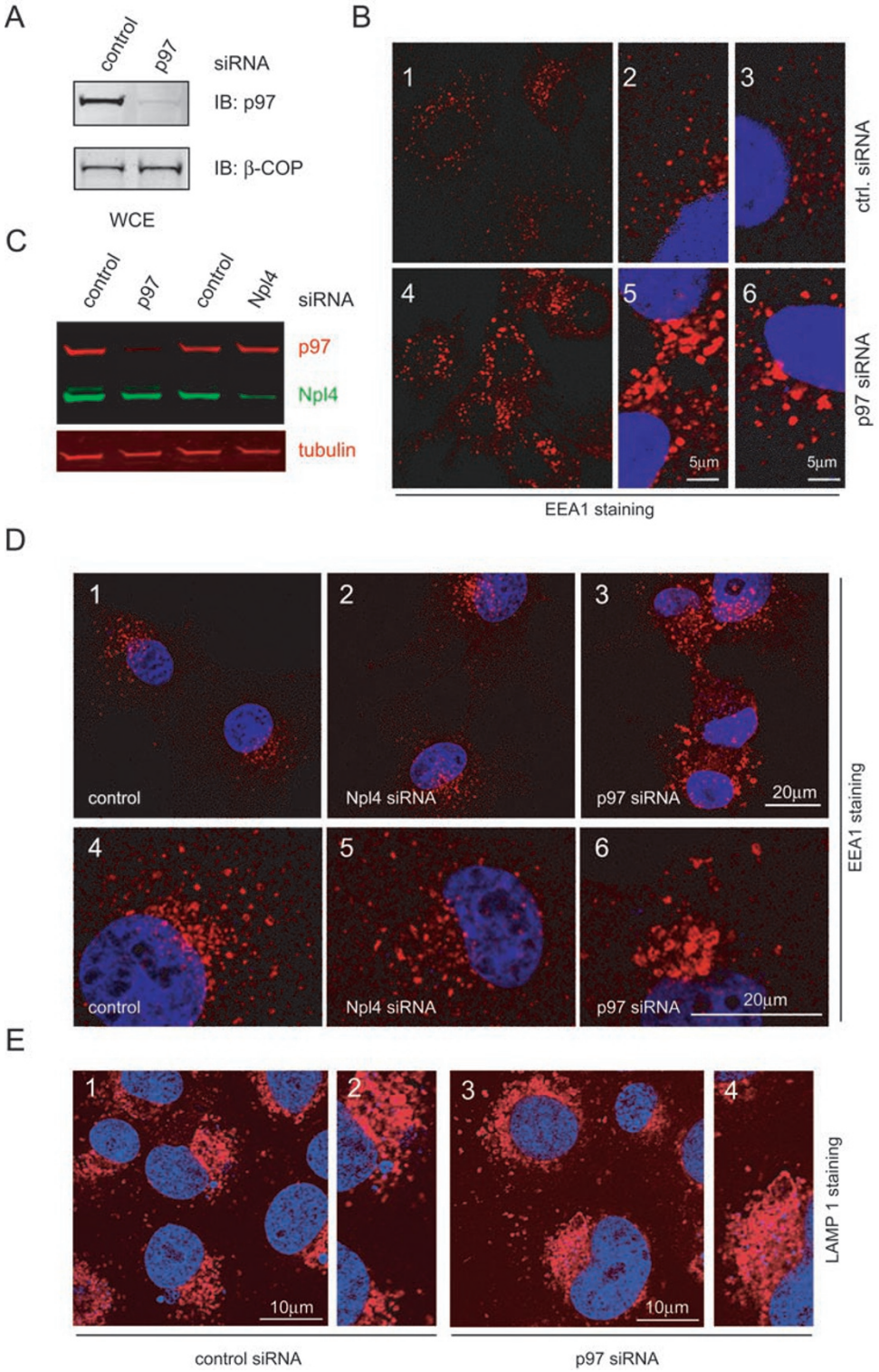

Figure 3 The p97 knockdown results in over-tethering/enlargement of early endosomes. **(A)** COS7 cells were treated with control or p97 specific siRNA. Whole cell extracts were subjected to immunoblotting to verify the knockdown efficiency. **(B)** Cells treated with control (panels 1, 2 and 3) or p97 specific siRNA (panels 4, 5 and 6) were immunostained to label endogenous EEA1 in red and DNA in blue. Panels 2, 3, 5 and 6 are close-up views of the cells. **(C)** COS7 cells were treated with control or p97-specific siRNA. Whole cell extracts were subjected to immunoblotting analysis with the indicated antibodies. **(D)** As in **B**, except that cells treated with the Npl4 siRNA were also included. Panels 4-6 are close-up views of the cells. **(E)** As in **B**, except that cells were stained with a LAMP1 antibody.

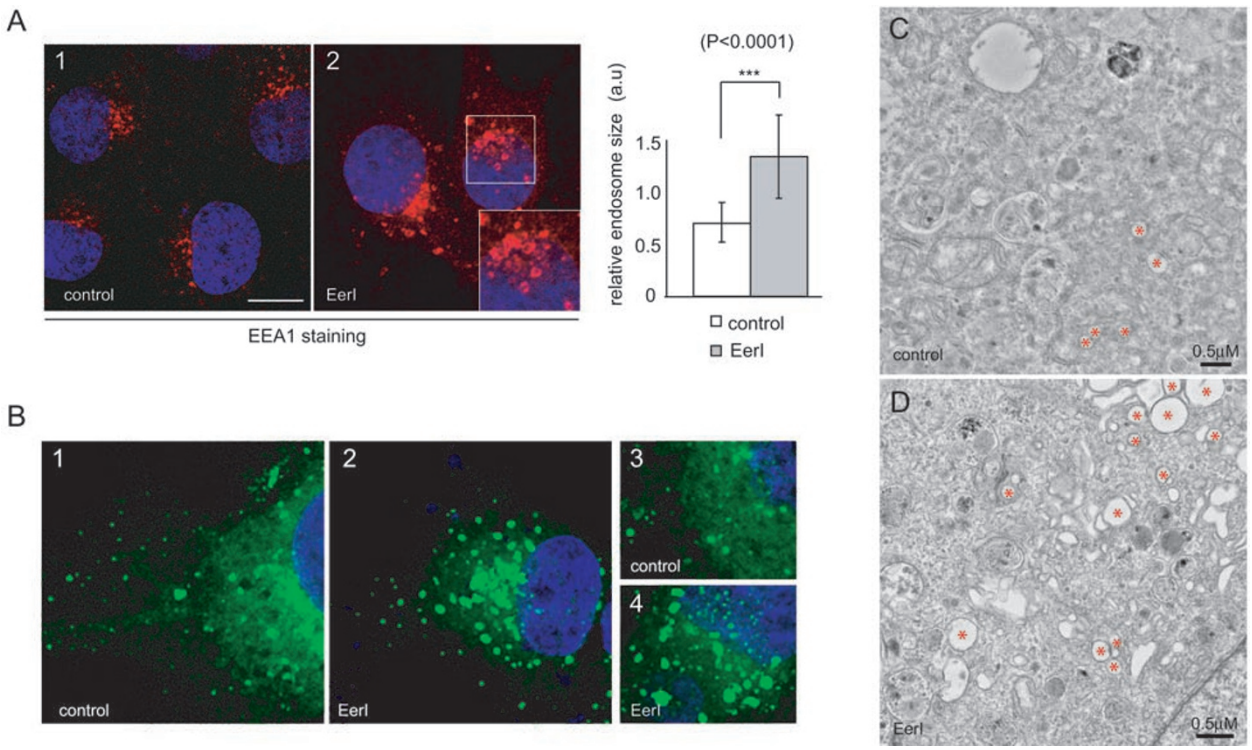

Figure 4 A p97 inhibitor causes enlargement of early endosomes. **(A)** COS7 cells treated with DMSO (control) or EerI (10 μM) for 6 h were stained for EEA1 in red and DNA in blue. The inset shows an enlarged view of the indicated region. Unless otherwise specified, scale bars correspond to 20 μm. The graph shows the quantification of the relative size of early endosomes in control and EerI-treated COS7 cells. a.u. arbitrary unit. Each value is the mean of 100 different vesicles, and the error bars represent the standard deviation. The *p*-value is obtained through paired *t*-test. **(B)** COS7 cells transfected with a low concentration of a Rab5-GFP-expressing plasmid were treated with either DMSO or EerI (10 μM) for 4 h. Cells were fixed and stained with DAPI. **(C**, **D)** COS7 cells treated with DMSO (**C**) or 10 μM EerI (**D**) for 4 h were fixed and analyzed by a transmission electron microscope at 4 000× magnification. Asterisks indicate examples of endosomes that are identified based on their unique membrane projections and lack of internal electron density [47].

region by 30 min (Figure 5A upper panels). In contrast, in EerI-treated cells, Tfn internalization occurred normally. However, after 30 min of chase, most cells did not display the perinuclear enrichment of Tfn-containing vesicles. Instead, Tfn was observed as punctate stains distributed throughout the cytoplasm (Figure 5A, lower panels). When the chase period was increased to 60 min, control cells contained few Tfn-positive vesicles due to recycling of Tfn. By contrast, most cells treated with EerI contained Tfn-positive vesicles that were clustered around a perinuclear region (Figure 5B). Thus, we conclude that p97 inhibition delays the intracellular trafficking of Tfn.

The p97 does not regulate EEA1-endosome interaction

Since p97 has been demonstrated to function as a "segregase" to dislocate polypeptides from large immobile entities such as the ER [4, 34] and the chromatin [7], we initially hypothesized that p97 might control the size of endosomes by dislocating components required for endosome fusion from the membrane. Given the demonstrated EEA1-p97 interaction and the finding that the EEA1 staining signal was enhanced in cells lacking functional p97, we suspected that p97 might regulate EEA1 localization. We thus examined the level of EEA1 on the endosome membrane relative to that in the cytosol in cells treated with EerI by a biochemical fractionation experiment. Surprisingly, when compared with control cells, p97 inhibition by EerI affected neither the total EEA1 levels nor the amount of EEA1 bound to endosomes (Figure 6A). Similarly, depletion of p97 by siRNA did not affect the level of membrane-bound EEA1 (Figure 6B). Thus, p97 does not seem to regulate EEA1 binding to the endosome membrane.

Inhibition of p97 causes increased EEA1 oligomerization

We then considered an alternative possibility. In this scenario, p97 might regulate the oligomeric state of

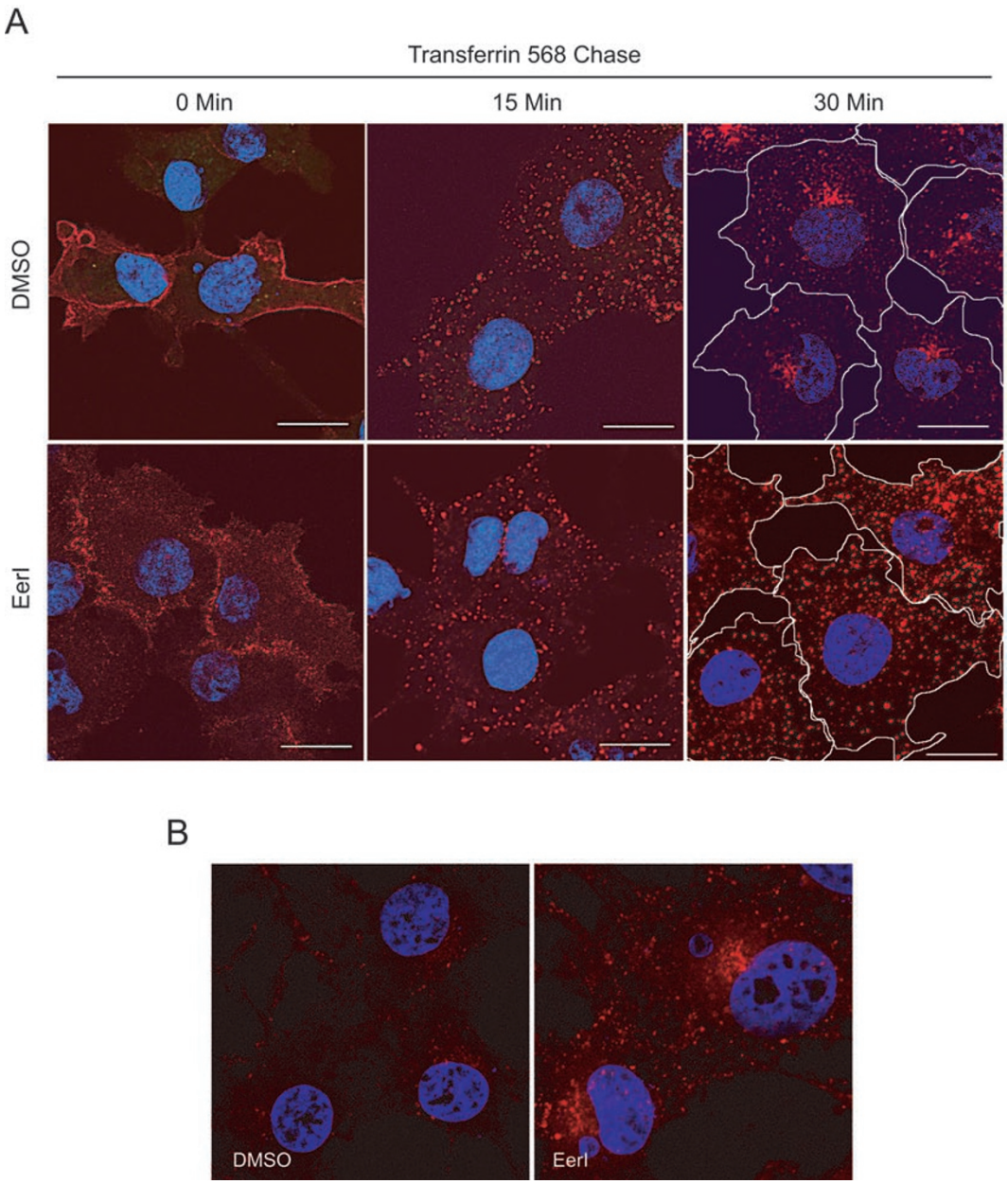

Figure 5 Inhibition of p97 delays the trafficking of an endocytic cargo. **(A)** COS7 cells treated with DMSO or EerI (10 μM) for 1 h were labeled with Tfn and chased for 0, 15 and 30 min. Panels show the temporal distribution of Tfn in red relative to the nuclei in blue. In the 30 min panels, cell boundary is outlined in white. **(B)** As in **A**, except that cells chased for 60 min are shown. Note that in control cells, few Tfn-containing vesicles are detected due to recycling of Tfn.

EEA1. We postulated that when p97 function was inhibited, there might be more oligomerized EEA1 on the endosome membrane, which could cause increased fluorescence staining due to enhanced antibody binding avidity. This would not affect the level of membrane-bound EEA1. EEA1 was reported to form a parallel dimer in cells [28, 29], which was proposed to be the functional unit of an EEA1 tethering complex. Thus, more EEA1 dimerization could explain the increased endosome clustering and enlargement phenotype associated with the loss of p97 function.

To monitor the level of EEA1 oligomerization, we first used a cysteine reactive crosslinker to stabilize the EEA1 dimer that would otherwise be disrupted during cell lysis and electrophoresis. COS7 cells exposed to either EerI or DMSO for 4 h were treated with BMH for additional

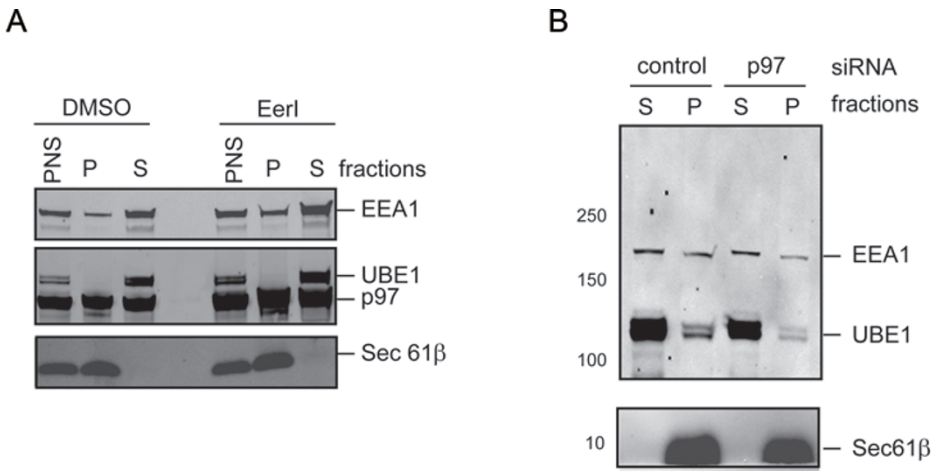

Figure 6 The p97 does not regulate EEA1 membrane association. **(A)** COS7 cells treated with DMSO or EerI for 4 h were fractionated into membrane (P) and cytosolic (S) fractions. The relative distribution of the indicated proteins was analyzed by immunoblotting. **(B)** As in **A**, except that control and p97 knockdown cells were used.

20 min on ice. Whole cell extracts were analyzed by immunoblotting. In control cells treated with 10μM BMH, SDS-resistant EEA1-containing high-molecular-weight complex could be detected and the EEA1 monomer level was reduced (Figure 7A, lane 3 versus 1). Treatment with 25 μM BMH generated more EEA1 high-molecular-weight complex with concomitant loss of the EEA1 monomer (lane 5). In EerI-treated cells, a significant increase in EEA1-containing high-molecular-weight complex was evident (Figure 7A, lanes 4 and 6 versus 3 and 5).

The EEA1-containing high-molecular-weight complexes might constitute both EEA1 homodimer as well as EEA1 heterooligomers that contained other EEA1-interacting proteins. These complexes had different mobility on SDS-PAGE gel, causing a smear-like immunoblotting signal. To see whether inhibition of p97 increased EEA1 self-association, we took a different approach. We postulated that since the EEA1-containing high-molecular-weight complexes can be stabilized by a homo-bifunctional cysteine crosslinker, the EEA1 homodimer present in the crosslinked complex mixture should contain two or more proximal cysteine residues from each monomer. In principle, disulfide bond should be formed between these cysteine residues when EEA1 is placed in a non-reducing environment (e.g. when cells are lysed in a buffer lacking any reducing or akylating reagents), and the extent of *de novo* disulfide formation during purification of EEA1 should correlate to the level of EEA1 dimerization in cells. This was indeed proven to be true for a mutant form of the T-cell receptor α chain that contains several pairs of proximal cysteine residues [42]. The level of such *in vitro*-generated disulfide dimer should appear homogenous when analyzed by immunoblotting. To this end, EEA1 was immunoprecipitated from cell extracts in the absence of any crosslinkers. Immunoblotting under the non-reducing conditions showed that a small fraction of EEA1 isolated from control cells migrated on a SDS-PAGE gel as a double-band with apparent molecular weight of ~500 kD (Figure 7B, lane 1). A similar doublet pattern was detected for EEA1 that was purified from cells overexpressing EEA1 (Figure 7C). Since recombinant EEA1 was purified to more than 90% homogeneity (Figure 7C, left panel), the disulfide-linked complex could only be produced by EEA1 self-association. The size of these species indicated that they likely represented distinct EEA1 homodimers linked by different cysteine residues, which often show altered protein mobility on SDS-PAGE gel as previously reported for other proteins [43]. Consistent with our hypothesis that EEA1 oligomerization enhanced antibody recognition, the EEA1 homodimer band appeared stronger than the monomer band on the blot although same amount of proteins were analyzed (Figure 7C). Interestingly, purified EEA1 proteins were mostly disulfide-bonded (Figure 7C, right panel), suggesting that the majority of overexpressed EEA1 existed in cells as a homodimer. This was further confirmed by a co-IP experiment using EEA1 variants carrying different epitope tags (Supplementary information, Figure S5A). Consistent with our idea that EEA1 self-association promoted endosome fusion, cells overexpressing EEA1 contained many enlarged endosomes (Supplementary Figure S5B-S5D). Moreover, similar to the BMH crosslinking result, more

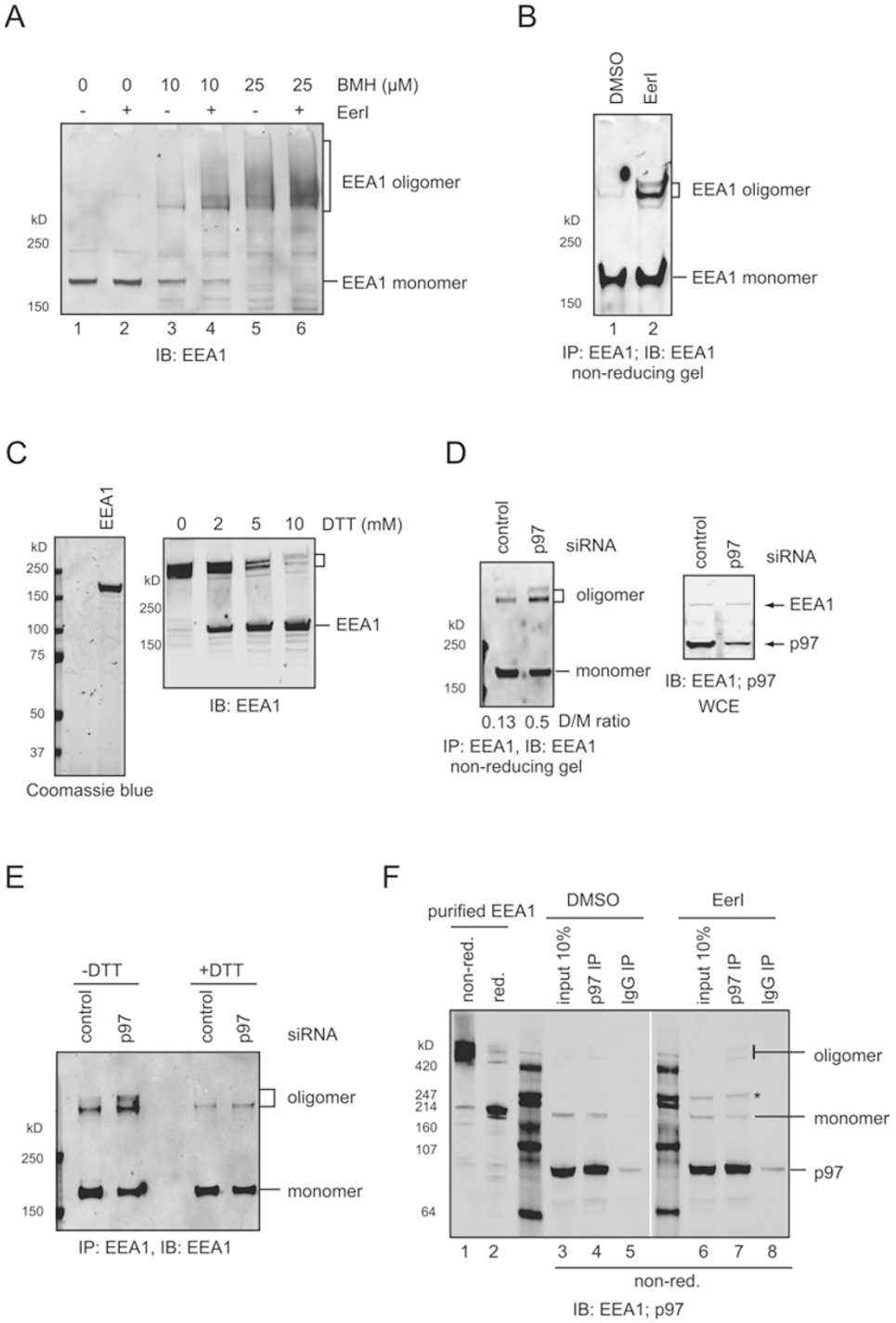

Figure 7 Inhibition of p97 increases EEA1 self-association. **(A)** COS7 cells exposed to 10 μM EerI or DMSO for 4 h were treated by the indicated concentrations of BMH. WCE was analyzed by immunoblotting. **(B)** EEA1 was immunoprecipitated from detergent extracts of EerI- or DMSO-treated COS7 cells and analyzed by immunoblotting under a non-reducing condition. **(C)** Purified EEA1 was analyzed by SDS-PAGE under the reducing condition (left panel). Purified EEA1 that has been treated with the indicated concentration of the reducing agent DTT was analyzed by immunoblotting. **(D)** As in **B**, except that control and p97 knockdown cells were used. The bottom panel shows the knockdown of p97 in p97 siRNA treated cells. The numbers in the right panel indicate the ratio of EEA1 dimer to the monomer (D/M). **(E)** As in **C**. Where indicated, a fraction of the precipitated EEA1 was analyzed under the reducing condition (+DTT). **(F)** EEA1 co-immunoprecipitated with p97 from the indicated cells was analyzed by immunoblotting under the non-reducing condition (non-red.). Lanes 1 (non-reducing) and 2 (reducing) show purified EEA1 protein for comparison. The asterisk indicates a p97 oligomeric species present in EerI-treated cells [38].

disulfide-linked EEA1 homooligomer could be detected in cell extract derived from EerI-treated cells (Figure 7B, lane 2 versus lane 1). Depletion of p97 by siRNA also increased the level of oligomerized EEA1 (Figure 7D). As expected, the disulfide-linked EEA1 dimer could be destabilized by the reducing agent DTT (Figure 7C and 7E). Importantly, when p97-associated pool of EEA1 was analyzed under the non-reducing condition, more oligomerized EEA1 was detected in association with p97 in EerI-treated cells than in control cells (Figure 7F, lane 7 versus lane 4). Together, these results suggest that p97 may regulate self-association of EEA1 to influence its tethering function.

Discussion

The p97 is an abundant ATPase that has many important cellular functions. In ERAD, p97 and its cofactors dislocate misfolded polypeptides into the cytosol for degradation by the proteasome [34, 44]. Here, we identify the early endosome fusion regulator EEA1 as a new substrate of p97. For EEA1, p97 does not function as a 'dislocase' to influence the interaction of EEA1 with the endosome membrane. Instead, our results suggest that p97 may govern the EEA1 oligomeric state to regulate endosome fusion and trafficking. This model is functionally distinct from the previously proposed role of p97 in regulating membrane fusion by acting on a SNARE complex comprising of Syntaxin-5 [12]. In the latter case, disassembly of the SNARE complex by p97 fuels the fusion reaction by regenerating free SNARE molecules, which can be used to support additional rounds of membrane fusion. By contrast, inhibition of EEA1 dimerization by p97 blocks membrane fusion because it reduces the levels of functional EEA1 tethering complex that is required for efficient membrane fusion.

The EEA1 dimer was reported to enter a high-molecular-weight hetero-oligomeric complex that includes NSF, Rab5, and some other Rab5 effectors such as Rabaptin-5 and Rabex-5, and this oligomeric EEA1 assembly is required for transient recruitment of syntaxin-13, which drives the membrane fusion reaction [24]. Interestingly, the EEA1 hetero-oligomeric assembly was shown to be modulated by NSF, which is required for the fusion reaction [24]. In light of these findings, we propose that the assembly of an EEA1-containing fusion complex might be subject to regulations by both p97 and NSF, the timing of which could produce opposing functional outcomes. NSF may dissociate EEA1 dimer from the rest of the fusion complex after the fusion machinery is properly recruited and fully assembled. At this time, the removal of the long rigid EEA1 dimer from the fusion complex may allows two vesicles to get close to each other, which facilitates the fusion reaction. On the other hand, p97 may act on EEA1 dimer prior to the recruitment of the fusion machinery. The p97 may use the energy from ATP hydrolysis to actively disassemble an EEA1 parallel dimer. Alternatively, it may bind an EEA1 monomer to inhibit the dimerization process. Our results favor the first model because when p97 function is inhibited, more unassembled EEA1 oligomer is detected in association with p97. Thus, it is possible that p97 may recognize oligomerized EEA1 to actively disassemble this complex, which reduces the level of functional EEA1 tethering complex and therefore attenuates endosome tethering and fusion.

The mechanism by which p97 recognizes EEA1 is unclear. *In vitro* binding experiment suggests that p97 does not bind EEA1 directly. Thus, like other p97 substrates, the recruitment of EEA1 to p97 likely involves a p97 cofactor. Our results do not support the involvement of Ufd1-Npl4 or p47 in p97-dependent endocytic regulation because overexpression of these factors in cells fails to increase the association of p97 with EEA1. Furthermore, most p97 substrates have been reported to undergo polyubiquitination in cells and many p97 cofactors contain ubiquitin-binding motifs that facilitate the interaction of p97 with polyubiquitinated substrates. Interestingly, we find that EEA1 is only monoubiquitinated at several lysine residues in cells (data not shown). Whether this modification participates in the newly established interplay between p97 and EEA1 is unclear. However, the fact that EEA1 is only monoubiquitinated further excludes the Ufd1-Npl4 complex and p47 as the mediator of p97-EEA1 interaction because these factors were reported to preferentially bind polyubiquitinated proteins [44, 45].

Preventing endosome overtethering/fusion might be important for cargo trafficking because a delay in endocytic trafficking was observed in cells treated with a p97 inhibitor. It is possible that endosome overtethering might affect its motility due to an altered interaction with the microtubule. Further studies are required to elucidate the mechanism by which endosome tethering and mobility are regulated.

Materials and Methods

Cell culture, plasmid preparation, transfection and RNAi

COS7, HeLa and 293T cells were purchased from ATCC. Full-length human EEA1 was purchased (OriGene). EEA1 deletion mutants were made by introducing SgfI or MluI sites at desired positions using PCR based site-directed mutagenesis. Restriction digestion using MluI or SgfI and religation yielded desired deletion mutants (Supplementary information, Table S1).

TransIT-293 (Mirus) and FuGENE 6 (Roche) were used for plasmid transfection. For siRNA-delivery into COS7 and 293T cells, DharmaFECT 2 and DharmaFECT 1 (Dharmacon

Inc) respectively, were used. ON-TARGETplus p97 siRNAs (CAAAUUGGCUGGUGAGUCU and CCUGAUUGCUCGAGCUGUA, respectively) and non-targeting control siRNA pool (D-001810-10) or Npl4-targeting siRNA pool (L-020796-01) was from Dharmacon. The 100 nM siRNA was transfected on 2 consecutive days and the knockdown analyses were performed 72 h post-first transfection.

Purification of EEA1

To purified EEA1, 293T cells were transfected with a plasmid expressing FLAG-tagged full-length EEA1. Cells were harvested 72 h post transfection in a buffer containing 1% DeoxyBig CHAP, 30 mM Tris HCl pH 7.4, 150 mM potassium acetate, 4 mM magnesium acetate and a protease inhibitor cocktail. The cleared cell extract was incubated with FLAG-agarose beads (Sigma) and the bound materials were extensively washed with a buffer containing 0.1% DeoxyBig CHAP, 30 mM Tris HCl pH 7.4, 150 mM potassium acetate and 4 mM magnesium acetate. The bound materials were eluted using 0.2 mg/ml 3× FLAG peptide (Sigma) in 25 mM Hepes, pH 7.2, 115 mM potassium acetate, 5 mM sodium acetate and 2.5 mM magnesium acetate.

Antibodies and chemicals

Rabbit anti-EEA1 (Cell Signaling), rabbit anti-LAMP1 (Santa Cruz Biotechnology), rabbit anti-Flag (Sigma), mouse anti-EEA1 (BD Biosciences), mouse anti-p97 antibody (Fitzgerald) and mouse anti-UBE1 (Thermoscientific) were used. Rabbit anti-p97 antibody was described previously [46]. Rabbit anti-Npl4 antibody was generated using a mixture of two peptides as antigen. The sequences of the peptides are as follows:

1 (C)DTRKGTVRYSRNKD

2 (C)SKQDGKIYRSRDPQ

Transferrin-568, goat anti-mouse or goat anti-rabbit conjugated to Alexa-568 and Alexa-488 were from Invitrogen. Goat anti-mouse conjugated to infrared dye IR680 and goat anti-rabbit conjugated to IR800 were from Rockland (Rockville, MD). EerI was synthesized by the chemical core of NIDDK. BMH was purchased from Pierce.

Crosslinking, immunoprecipitation and cell fractionation

Cells in a six-well plate were washed once with the crosslinking buffer (10 mM Hepes 7.4, 10 mM glucose, 100 mM NaCl, 1.2 mM $CaCl_2$, 1.2 mM $MgCl_2$ and 50 mM KCl) and incubated for 20 min on ice with the cysteine-specific crosslinker 1, 4-bis-maleimidohexane (BMH) at either 10 or 25 μM. Cells were washed twice with PBS, lysed in a lysis buffer (50 mM Tris HCl pH 8.0, 5 mM $MgCl_2$, 150mM NaCl and 0.6% Igepal CA-630), and extracts were analyzed by immunoprecipitation and/or immunoblotting according to standard procedures.

For membrane fractionation experiments, cells from a 15 cm dish were dounce homogenized in a hypotonic buffer (50 mM Hepes, 7.3, 10 mM potassium chloride, 2 mM magnesium chloride and a protease inhibitor cocktail) and centrifuged for 5 min at 1 000× *g* to remove the unbroken cells and nuclei. The resulting post-nuclear supernatant is subjected to centrifugation at 75 000 rpm for 20 min in a TLA120 rotor to pellet the total membranes. The membranes are then resuspended in the HM buffer (50 mM Hepes, 7.3, 3 mM imidazole and protease inhibitors) and mixed with 80% sucrose made in HM buffer to obtain membrane suspension with 50% sucrose. This was placed at the bottom of a TLA120 ultracentrifugation tube, which was overlayed with 40% and 25% sucrose step-gradients and centrifuged at 110 kg for 1 h. Fractions were collected from the top and analyzed by immunoblotting.

Confocal microscopy and electron microscope analyses

For EEA1 staining, cells plated on coverslips for 24 h were fixed in 2% formaldehyde in PBS for 10 min, rinsed in PBS and blocked for 15 min in PBS containing 10% FBS. Post blocking, the cells were rinsed and incubated with mouse or rabbit anti-EEA1 primary antibodies (1:100 dilution) in PBS containing 10% FBS and 0.2% saponin. For p97 staining, cells were fixed in 4% paraformaldehyde containing 250 mM sucrose, permeabilized and stained with mouse anti-p97 antibody in PBS containing 0.1% Igepal CA-630 and detected with secondary goat anti-mouse or goat anti-rabbit secondary antibodies conjugated to Alexa fluro-568 or 488. To track endocytic cargoes, cells were washed and starved for 30 min in serum-free DMEM containing 0.5% BSA followed by 15 min incubation with labeled Transferrin (5 μg/ml) on ice. The cells were washed twice with PBS and the bound labeled cargoes were allowed to internalize for different time points by incubating the cells at 37 °C. All images were obtained using a 510 LSM Confocal microscope (Zeiss) with a 100× Plan Apo objective and processed using Adobe Photoshop 7.0. The relative size of the endosomes was quantified using the LSM Image Browser 4.0. One hundred EEA1-containing vesicles from DMSO and EerI-treated cells were randomly selected from two independent staining experiments. We calculated the vesicle size by averaging the length and width of an individual vesicle. The mean and standard deviation of the vesicle sizes were then plotted as histograms and the significance was calculated using paired *T*-test. For electron microscope analyses, COS7 cells were treated with either DMSO or 10 μM EerI for 3 h. Cells were washed with PBS and then fixed with 2% glutaraldehyde in 0.1 M cacodylate buffer at room temperature for 1 h. The samples were examined in the Electron Microscope Laboratory at the National Cancer Institute.

Acknowledgments

We thank J Donaldson (NHLBI) for reagents and valuable suggestions, T Rapoport for the Sec61β antibody, B Baibakov (NIDDK) for assistance with the confocal microscopy, C M Burks (NCI) for performing the EM analyses, J Donaldson (NHLBI) and H Bernstein (NIDDK) for critical reading of the manuscript. The research is supported by the NIH Intramural AIDS Targeted Antiviral Program (IATAP) and by the Intramural Research Program of the NIDDK.

References

1 DeLaBarre B, Brunger AT. Complete structure of p97/valosin-containing protein reveals communication between nucleotide domains. *Nat Struct Biol* 2003; **10**:856-863.

2 Zhang X, Shaw A, Bates PA, *et al*. Structure of the AAA ATPase p97. *Mol Cell* 2000; **6**:1473-1484.

3 Jentsch S, Rumpf S. Cdc48 (p97): a "molecular gearbox" in the ubiquitin pathway? *Trends Biochem Sci* 2007; **32**:6-11.

4 Ye Y. Diverse functions with a common regulator: ubiquitin takes command of an AAA ATPase. *J Struct Biol* 2006;

156:29-40.
5 Wilcox AJ, Laney JD. A ubiquitin-selective AAA-ATPase mediates transcriptional switching by remodelling a repressor-promoter DNA complex. *Nat Cell Biol* 2009; **11**:1481-1486.
6 Mouysset J, Deichsel A, Moser S, *et al*. Cell cycle progression requires the CDC-48UFD-1/NPL-4 complex for efficient DNA replication. *Proc Natl Acad Sci USA* 2008; **105**:12879-12884.
7 Ramadan K, Bruderer R, Spiga FM, *et al*. Cdc48/p97 promotes reformation of the nucleus by extracting the kinase Aurora B from chromatin. *Nature* 2007; **450**:1258-1262.
8 Bays NW, Hampton RY. Cdc48-Ufd1-Npl4: stuck in the middle with Ub. *Curr Biol* 2002; **12**:R366-R371.
9 Latterich M, Frohlich KU, Schekman R. Membrane fusion and the cell cycle: Cdc48p participates in the fusion of ER membranes. *Cell* 1995; **82**:885-893.
10 Kano F, Kondo H, Yamamoto A, *et al*. NSF/SNAPs and p97/p47/VCIP135 are sequentially required for cell cycle-dependent reformation of the ER network. *Genes Cells* 2005; **10**:989-999.
11 Uchiyama K, Jokitalo E, Kano F, *et al*. VCIP135, a novel essential factor for p97/p47-mediated membrane fusion, is required for Golgi and ER assembly *in vivo*. *J Cell Biol* 2002; **159**:855-866.
12 Rabouille C, Kondo H, Newman R, Hui N, Freemont P, Warren G. Syntaxin 5 is a common component of the NSF- and p97-mediated reassembly pathways of Golgi cisternae from mitotic Golgi fragments *in vitro*. *Cell* 1998; **92**:603-610.
13 Uchiyama K, Totsukawa G, Puhka M, *et al*. p37 is a p97 adaptor required for Golgi and ER biogenesis in interphase and at the end of mitosis. *Dev Cell* 2006; **11**:803-816.
14 Meyer HH. Golgi reassembly after mitosis: the AAA family meets the ubiquitin family. *Biochim Biophys Acta* 2005; **1744**:108-119.
15 Meyer HH, Shorter JG, Seemann J, Pappin D, Warren G. A complex of mammalian ufd1 and npl4 links the AAA-ATPase, p97, to ubiquitin and nuclear transport pathways. *EMBO J* 2000; **19**:2181-2192.
16 Pleasure IT, Black MM, Keen JH. Valosin-containing protein, VCP, is a ubiquitous clathrin-binding protein. *Nature* 1993; **365**:459-462.
17 Mu FT, Callaghan JM, Steele-Mortimer O, *et al*. EEA1, an early endosome-associated protein. EEA1 is a conserved alpha-helical peripheral membrane protein flanked by cysteine "fingers" and contains a calmodulin-binding IQ motif. *J Biol Chem* 1995; **270**:13503-13511.
18 Ohya T, Miaczynska M, Coskun U, *et al*. Reconstitution of Rab- and SNARE-dependent membrane fusion by synthetic endosomes. *Nature* 2009; **459**:1091-1097.
19 Stenmark H, Aasland R, Toh BH, D'Arrigo A. Endosomal localization of the autoantigen EEA1 is mediated by a zinc-binding FYVE finger. *J Biol Chem* 1996; **271**:24048-24054.
20 Simonsen A, Lippe R, Christoforidis S, *et al*. EEA1 links PI(3)K function to Rab5 regulation of endosome fusion. *Nature* 1998; **394**:494-498.
21 Callaghan J, Nixon S, Bucci C, Toh BH, Stenmark H. Direct interaction of EEA1 with Rab5b. *Eur J Biochem* 1999; **265**:361-366.
22 Zerial M, McBride H. Rab proteins as membrane organizers. *Nat Rev Mol Cell Biol* 2001; **2**:107-117.
23 Stenmark H. Rab GTPases as coordinators of vesicle traffic. *Nat Rev Mol Cell Biol* 2009; **10**:513-525.
24 McBride HM, Rybin V, Murphy C, Giner A, Teasdale R, Zerial M. Oligomeric complexes link Rab5 effectors with NSF and drive membrane fusion via interactions between EEA1 and syntaxin 13. *Cell* 1999; **98**:377-386.
25 Christoforidis S, McBride HM, Burgoyne RD, Zerial M. The Rab5 effector EEA1 is a core component of endosome docking. *Nature* 1999; **397**:621-625.
26 Gaullier JM, Simonsen A, D'Arrigo A, Bremnes B, Stenmark H. FYVE finger proteins as effectors of phosphatidylinositol 3-phosphate. *Chem Phys Lipids* 1999; **98**:87-94.
27 Kutateladze TG, Ogburn KD, Watson WT, *et al*. Phosphatidylinositol 3-phosphate recognition by the FYVE domain. *Mol Cell* 1999; **3**:805-811.
28 Dumas JJ, Merithew E, Sudharshan E, *et al*. Multivalent endosome targeting by homodimeric EEA1. *Mol Cell* 2001; **8**:947-958.
29 Callaghan J, Simonsen A, Gaullier JM, Toh BH, Stenmark H. The endosome fusion regulator early-endosomal autoantigen 1 (EEA1) is a dimer. *Biochem J* 1999; **338 (Pt 2)**:539-543.
30 Li L, Hailey DW, Soetandyo N, *et al*. Localization of A20 to a lysosome-associated compartment and its role in NFkappaB signaling. *Biochim Biophys Acta* 2008; **1783**:1140-1149.
31 Rybin V, Ullrich O, Rubino M, *et al*. GTPase activity of Rab5 acts as a timer for endocytic membrane fusion. *Nature* 1996; **383**:266-269.
32 Buchberger A. Control of ubiquitin conjugation by cdc48 and its cofactors. *Subcell Biochem* 2011; **54**:17-30.
33 Bruderer RM, Brasseur C, Meyer HH. The AAA ATPase p97/VCP interacts with its alternative co-factors, Ufd1-Npl4 and p47, through a common bipartite binding mechanism. *J Biol Chem* 2004; **279**:49609-49616.
34 Ye Y, Meyer HH, Rapoport TA. The AAA ATPase Cdc48/p97 and its partners transport proteins from the ER into the cytosol. *Nature* 2001; **414**:652-656.
35 Kondo H, Rabouille C, Newman R, *et al*. p47 is a cofactor for p97-mediated membrane fusion. *Nature* 1997; **388**:75-78.
36 Magadan JG, Perez-Victoria FJ, Sougrat R, Ye Y, Strebel K, Bonifacino JS. Multilayered mechanism of CD4 downregulation by HIV-1 Vpu involving distinct ER retention and ERAD targeting steps. *PLoS Pathog* 2010; **6**:e1000869.
37 Ballar P, Pabuccuoglu A, Kose FA. Different p97/VCP complexes function in retrotranslocation step of mammalian Er-associated degradation (ERAD). *Int J Biochem Cell Biol* 2011; **43**:613-621.
38 Wang Q, Shinkre BA, Lee JG, *et al*. The ERAD inhibitor Eeyarestatin I is a bifunctional compound with a membrane-binding domain and a p97/VCP inhibitory group. *PLoS One* 2011; **5**:e15479.
39 Bucci C, Parton RG, Mather IH, *et al*. The small GTPase rab5 functions as a regulatory factor in the early endocytic pathway. *Cell* 1992; **70**:715-728.
40 Gorvel JP, Chavrier P, Zerial M, Gruenberg J. rab5 controls early endosome fusion *in vitro*. *Cell* 1991; **64**:915-925.
41 Stenmark H, Parton RG, Steele-Mortimer O, Lutcke A, Gruenberg J, Zerial M. Inhibition of rab5 GTPase activity stimulates membrane fusion in endocytosis. *EMBO J* 1994;

13:1287-1296.

42 Soetandyo N, Wang Q, Ye Y, Li L. Role of intramembrane charged residues in the quality control of unassembled T-cell receptor alpha-chains at the endoplasmic reticulum. *J Cell Sci* 2010; **123**:1031-1038.

43 Carvalho P, Stanley AM, Rapoport TA. Retrotranslocation of a misfolded luminal ER protein by the ubiquitin-ligase Hrd1p. *Cell* 2011; **143**:579-591.

44 Ye Y, Meyer HH, Rapoport TA. Function of the p97-Ufd1-Npl4 complex in retrotranslocation from the ER to the cytosol: dual recognition of nonubiquitinated polypeptide segments and polyubiquitin chains. *J Cell Biol* 2003; **162**:71-84.

45 Meyer HH, Wang Y, Warren G. Direct binding of ubiquitin conjugates by the mammalian p97 adaptor complexes, p47 and Ufd1-Npl4. *EMBO J* 2002; **21**:5645-5652.

46 Ye Y, Shibata Y, Kikkert M, van Voorden S, Wiertz E, Rapoport TA. Inaugural Article: Recruitment of the p97 ATPase and ubiquitin ligases to the site of retrotranslocation at the endoplasmic reticulum membrane. *Proc Natl Acad Sci USA* 2005; **102**:14132-14138.

47 Wegner CS, Malerod L, Pedersen NM, *et al*. Ultrastructural characterization of giant endosomes induced by GTPase-deficient Rab5. *Histochem Cell Biol* 2009; **133**:41-55.

(**Supplementary information** is linked to the online version of the paper on the *Cell Research* website.)